J Supercond Nov Magn (2009) 22: 247–250
DOI 10.1007/s10948-008-0426-9

ORIGINAL PAPER

Properties of high-T_C Copper Oxides from Band Models of Spin–Phonon Coupling

T. Jarlborg

Received: 10 December 2008 / Accepted: 12 December 2008 / Published online: 6 January 2009

Abstract The mechanism of spin–phonon coupling (SPC) and possible consequences for the properties of high-T_C copper oxides are presented. The results are based on ab initio LMTO band calculations and a nearly free-electron (NFE) model of the band near E_F. Many observed properties are compatible with SPC, as for the relation between doping and $\vec{q}$ for spin excitations and their energy dependence. The main pseudogap is caused by SPC and waves along [1, 0, 0], but it is suggested that secondary waves, generated along [1, 1, 0], contribute to a 'waterfall' structure. Conditions for optimal T_C, and the possibilities for spin enhancement at the surface are discussed.

Keywords High-T_C superconductivity · Spin excitations · Band structure · Waterfalls · Surface magnetism

PACS 74.25.Jb · 74.20.-z · 74.20.Mn · 74.72.-h

1 Introduction

The normal state properties of high-T_C copper oxides show many unusual properties like pseudogaps, stripe-like charge/spin modulations with particular energy and doping dependencies, Fermi-surface (FS) "arcs" in the diagonal direction, 'kinks' and 'waterfalls' (WF) in the band dispersions, manifestations of isotope shifts, phonon softening, and so on [1–10]. Band results for long '1-dimensional' (1-D) supercells, calculated by the Linear Muffin-Tin Orbital (LMTO) method and the local spin-density approximation (LDA), show large spin–phonon coupling (SPC) within the CuO plane of these systems [11]. This means that an antiferromagnetic (AFM) wave of the correct wave length and the proper phase is stronger when it coexists with the phonon [12]. The LMTO results have been used to parameterize the strength of potential modulations coming from phonon distortions and spin waves of different length [13]. These parameters have been used in a nearly free-electron (NFE) model in order to visualize the band effects from the potential modulations in 2-D. Many properties are consistent with SPC, as have been shown previously [11–15].

T. Jarlborg (✉)
DPMC, University of Geneva, 24 Quai Ernest-Ansermet, 1211 Geneva 4, Switzerland
e-mail: Thomas.Jarlborg@unige.ch

2 Calculations and Results

Ab initio LMTO band calculations based on the local density approximation (LDA) are made for $La_{(2-x)}Ba_xCuO_4$ (LBCO), with the use of the virtual crystal approximation (VCA) to La-sites to account for doping, x. Calculations for long supercells, mostly oriented along the CuO bond direction, are used for modeling of phonon distortions and spin waves [13]. The calculations show that pseudogaps (a 'dip' in the density-of-states, DOS) appear at different energies depending on the wave lengths of the phonon/spin waves. This is consistent with a correlation between doping and wave length, and with phonon softening in doped systems [12].

The difficulty with ab initio calculations is that very large unit cells are needed for realistic 2D-waves. Another shortcoming is that the original Brillouin zone is folded by the use of supercells, which makes interpretation difficult. The band at E_F is free-electron like, with an effective mass near one, and the potential modulation and SPC can be studied within the nearly free-electron model (NFE) [14]. The AFM spin arrangement on near-neighbor (NN)

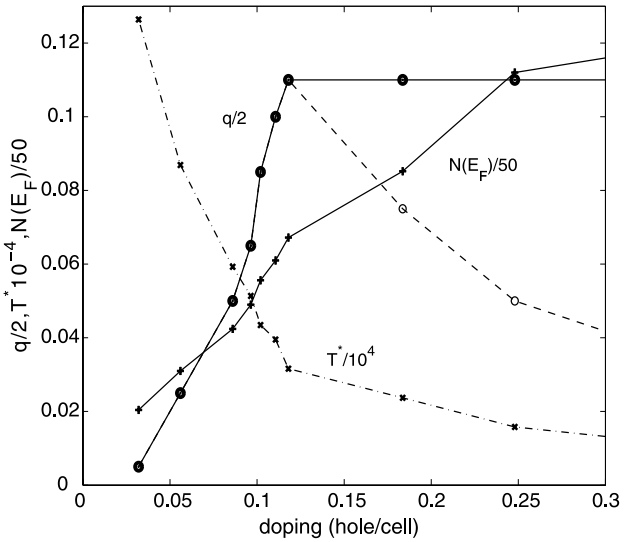

Fig. 1 The variation of magnetic modulation vector $q/2$ (*circles*), density-of-states in the pseudogap (+-signs $N(E_F)/50$ in states per cell/Ry/spin), and $T^*/10000$ (x-signs in K), as function of doping x in a NFE model with parameters from [14]. Two different q-vectors along q_x and q_y are needed for doping larger than about 0.12, as indicated by the filled and *open circles*

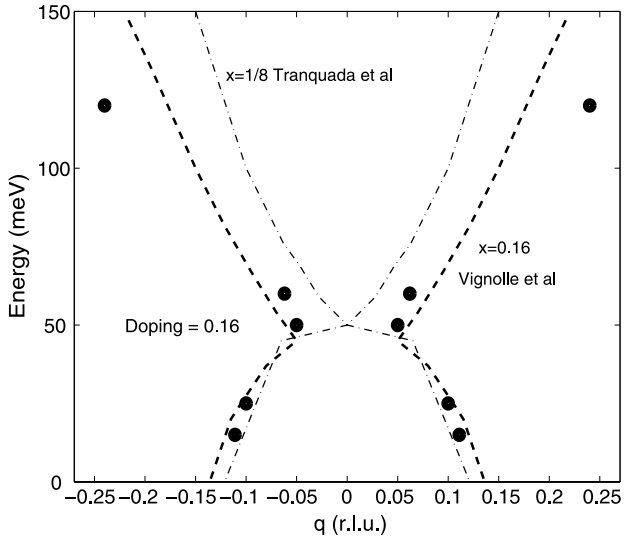

Fig. 2 Filled circles: Calculated $q - \hbar\omega$ relation from the 2D-NFE model and the parameters V_q^t for doping $x = 0.16$. The solution without SPC at the largest energy, is less precise. Broken line: Approximate shape of the experimental dispersion as it is read from Fig. 3**c** in the work of Vignolle et al. [10] for $La_{2-x}Sr_xCuO_4$ at $x = 0.16$. *Thin semi-broken line*: Experimental dispersion read from the data by Tranquada et al. [9] on LBCO at lower doping, $x = 0.125$

Cu along $[1, 0, 0]$ corresponds to a potential perturbation, $V(\bar{x}) = V_q^t \exp(-i\,\bar{Q}\cdot\bar{x})$ (and correspondingly for $\bar{y}$). A further modulation ($\bar{q}$) leads to 1D-stripes perpendicular to $\bar{x}$ (or "checkerboards" in 2-D along $\bar{x}$ and $\bar{y}$), with a modification; $V(\bar{x}) = V_q^t \exp(-i(\bar{Q} - \bar{q})\cdot\bar{x})$, and the gap moves from the zone boundary to $(\bar{Q} - \bar{q})/2$ [14].

The NFE model reproduces the qualitative results of the full band (1-D) calculation. In 2-D it leads to a correlation between doping and the amplitude of V_q^t, because the gap (at E_F) opens along $(k_x, 0)$ and $(0, k_y)$, but not along the diagonal [14]. The combined effect is that the dip in the total DOS (at E_F) will not appear at the same band filling for a small and a wide gap. The q vs. x behavior for a spherical NFE band with m^* close to 1, and parameters V_q^t (for one type of phonon) from ref. [14] show a saturation, see Fig. 1. This is quite similar to what has been observed [8]. The reason is that no checkerboard solutions are found for larger doping, but unequal $q_x/2$ (fixed near 0.11) and $q_y/2$ produce realistic solutions. The DOS at E_F, N, is lowest within the pseudogap. A gap caused by spin waves disappears at a temperature T^* when thermal excitations can overcome the gap, and the spin wave can no longer be supported. Therefore, the spin waves are most important for the pseudogap (even though phonons are important via SPC), and T^* is estimated to be 1/4th of the spin part of V_q^t [14]. The opposite x-variations of T^* and N (note that $\lambda \propto N V_q^2$) provide an argument for optimal conditions for superconductivity for intermediate x [14]. Moreover, the pseudogap competes with superconductivity at underdoping, since dynamic SPC would be their common cause. However, there is a possibility to raise N and T_C by creating an artificial, static pseudogap through a periodic distribution of dopants or strain. Two parameters, the periodicity and the strength of the perturbing potential, should be adjusted so that the peak in the DOS above or below the static pseudogap coincides with E_F.

The degree of SPC is different for different phonons. The total V_q^t with contributions from phonons and spin waves, calculated from LMTO and information from phonon calculations for Nd_2CuO_4 [16], are 17, 18, 23 and 22 mRy at energies centered around 15 (La), 25 (Cu), 50 (plane-O) and 60 meV (apical-O), respectively [15]. The results for $x = 0.16$ are shown in Fig. 2, together with experimental data [9, 10]. The points below 70 meV are for the coupling to the 4 types of phonons. The spectrum is shaped like an hourglass with a "waist" at intermediate energy with largest SPC for plane-O. The solutions for energies larger than 70 meV are independent of phonons and the exact (q, ω) behavior is more uncertain [15]. Less doping implies larger V_q^t and longer waves. All $\vec{q}$ become smaller and the waist becomes narrower, as can be verified in LBCO for $x = 1/8$ [9], and recently in lightly doped $La_{1.96}Sr_{0.04}CuO_4$ [4]. However, the spin modulation in the latter case is in the diagonal direction. Heavier O-isotopes will decrease the frequencies for the phonons and the coupled spin waves, and move the waist to lower E.

Another odd feature is the WF-dispersion of the band below E_F in the diagonal direction, seen by ARPES [3]. The suggestion here is that this feature comes from a gap be-

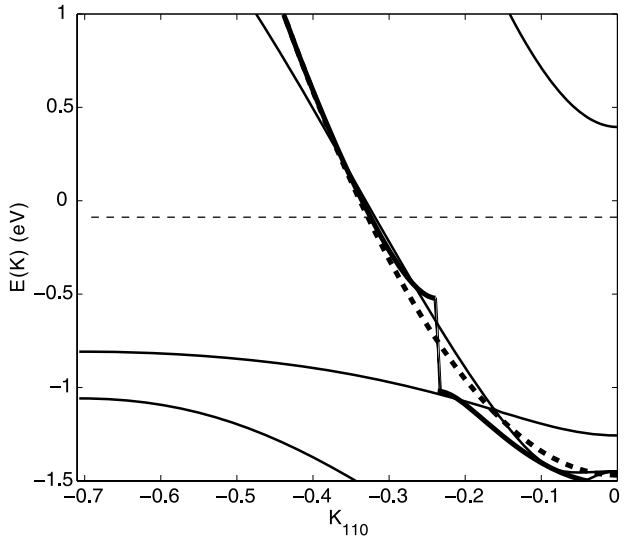

Fig. 3 *Thin lines*: LMTO band structure for LBCO between M and Γ. *Broken line*: the FE fit, and the *heavy line* the NFE solution with a gap. E_F is at zero in undoped LBCO, and at the *thin broken line* for $x \sim 0.15$

low E_F in the diagonal direction. An inspection of the potential for stripe modulations along $[1, 0, 0]$ reveals that the potential becomes modulated also along $[1, 1, 0]$, albeit in a different fashion. The potential is slowly varying like the absolute value of *sine*-functions with different phase along different rows. No NN-AFM potential shifts are found along $[1, 1, 0]$, and the dominant Cu-d lobes of wave function for $\vec{k}$ along $[1, 1, 0]$ are oriented along $[1, 1, 0]$ and not along the bond direction. Various arguments for the effective periodicity, partly based on these conditions, indicate that a gap should appear at about $1/3$ of the distance between Γ and the M point when the doping is near 0.16. The effective V_q should be less than half of the amplitude along $[1, 0, 0]$. The result is shown in Fig. 3. The k-position of the gap and the extreme values of the gap energies ($\sim$ 0.5–1 eV below E_F) are not too far from what is seen experimentally [3], but again, the quantitative power of the NFE model is limited. It is not clear if the vertical part of the band dispersion can be observed. A vertical line is connecting the states above and below the gap in Fig. 3, which could be justified for an imperfect gap away from the zone boundary.

The dynamics is important if SPC mediates superconductivity. But static, stripe-like features are identified by surface tunneling spectroscopy (STM) [17]. Impurities and defects near the surface might be important, but also the surface itself could modify the conditions for SPC. The latter hypothesis is investigated in LMTO calculations which simulate the surface through insertion of two layers of empty spheres between the outermost LaO layers. These calculations consider 3 and 5 layers of undoped La_2CuO_4, and 3 layers of a doped LBCO with and without phonon distortion in a cell of length $4a_0$ in the CuO bond direction. The SPC remains in the surface layer. The effective doping is in all cases found to increase close to the surface, which has 0.1–0.2 more electrons/Cu than the Cu in the interior, and the magnetic moment is 2–3 times larger in the surface layer. The moments disappear without field, but a calculation for 3 layers of La_2CuO_4 with a narrower separating layer, has stable AFM moments $\pm 0.06\mu_B$ per Cu within the surface layer, and the local DOS on the Cu at the surface drops near E_F. In addition, also the apical-O nearest to the surface acquires a sizable moment. This calculation is simplified, with a probable interaction across the empty layer, but it shows that static AFM surface configurations are very close to stability.

3 Conclusion

Band calculations show that SPC is important for waves along $[1, 0, 0]$ or $[0, 1, 0]$, with secondary effects in the diagonal direction. Many properties, like pseudogaps, phonon softening, dynamic stripes, correlation between $\bar{q}$ and x, smearing of the non-diagonal part of the FS, and abrupt disappearance of the spin fluctuations at a certain T^*, are possible consequences of SPC within a rather conventional band [13, 14]. Different SPC for different phonons leads to a hourglass shape of the (q, ω)-spectrum with the narrowest part for the modes with strongest coupling. The much discussed WF-structure in the diagonal band dispersion could be a result of a secondary potential modulation in this direction and a gap below E_F. Static potential modulations within the CuO-planes, such as for superstructures, could compensate the pseudogap and enhance $N(E_F)$ and T_C. Spin waves become softer through interaction with phonons and near the surface. These LDA results show a tendency for static spin waves at the surface.

References

1. Tranquada, J.M., Sternlieb, B.J., Axe, J.D., Nakamura, Y., Uchida, S.: Nature **375**, 561 (1995) and references therein
2. Damascelli, A., Shen, Z.-X., Hussain, Z.: Rev. Mod. Phys. **75**, 473 (2003) and references therein
3. Chang, J., Shi, M., Pailhes, S., Månson, M., Claesson, T., Tjernberg, O., Bendounan, A., Patthey, L., Momono, N., Oda, M., Ido, M., Mudry, C., Mesot, J.: cond-matt arXiv:0708.2782 (2007)
4. Matsuda, M., Fujita, M., Wakimoto, S., Fernandez-Baca, J.A., Tranquada, J.M., Yamada, K.: cond-matt arXiv:0801:2254v1 (2008)
5. Fukuda, T., Mizuki, J., Ikeuchi, K., Yamada, K., Baron, A.Q.R., Tsutsui, S.: Phys. Rev. B **71**, 060501(R) (2005)
6. Zhao, G.M., Keller, H., Conder, K.: J. Phys.: Cond. Mat. **13**, R569 (2001)
7. Gweon, G.-H., Sasagawa, T., Zhou, S.Y., Graf, J., Takagi, H., Lee, D.-H., Lanzara, A.: Nature **430**, 187 (2004)
8. Yamada, K., Lee, C.H., Kurahashi, K., Wada, J., Wakimoto, S., Ueki, S., Kimura, H., Endoh, Y., Hosoya, S., Shirane, G., Birgenau, R.J., Greven, M., Kastner, M.A., Kim, Y.J.: Phys. Rev. B **57**, 6165 (1998)

9. Tranquada, J.M., Woo, H., Perring, T.G., Goka, H., Gu, G.D., Xu, G., Fujita, M., Yamada, K.: Nature **429**, 534 (2004)
10. Vignolle, B., Hayden, S.M., McMorrow, D.F., Rönnow, H.M., Lake, B., Perring, T.G.: Nature Phys. **3**, 163 (2007)
11. Jarlborg, T.: Phys. Rev. B **64**, 060507(R) (2001)
12. Jarlborg, T.: Phys. Rev. B **68**, 172501 (2003)
13. Jarlborg, T.: Physica C **454**, 5 (2007)
14. Jarlborg, T.: Phys. Rev. B **76**, 140504(R) (2007)
15. Jarlborg, T.: cond-matt arXiv:0804.2403 (2008)
16. Chen, H., Callaway, J.: Phys. Rev. B **46**, 14321 (1992)
17. Kohsaka, Y., Taylor, C., Fujita, K., Schmidt, A., Lupien, C., Hanaguri, T., Azuma, M., Esaki, H., Takagi, H., Uchida, S., Davis, J.C.: Science **315**, 1380 (2007)